

Cite this: *Analyst*, 2015, **140**, 2540–2555

A gold nanorod-based localized surface plasmon resonance platform for the detection of environmentally toxic metal ions

Subramaniam Jayabal,^{*a} Alagarsamy Pandikumar,^a Hong Ngee Lim,^b Ramasamy Ramaraj,^{a,c} Tong Sun^d and Nay Ming Huang^{*a}

Gold nanorods (Au NRs) are elongated nanoparticles with unique optical properties which depend on their shape anisometry. The Au NR-based longitudinal localized surface plasmon resonance (longitudinal LSPR) band is very sensitive to the surrounding local environment and upon the addition of target analytes, the interaction between the analytes and the surface of the Au NRs leads to a change in the longitudinal LSPR band. This makes it possible to devise Au NR probes with application potential to the detection of toxic metal ions with an improved limit of detection, response time, and selectivity for the fabrication of sensing devices. The effective surface modification of Au NRs helps in improving their selectivity and sensitivity toward the detection of toxic metal ions. In this review, we discuss different methods for the preparation of surface modified Au NRs for the detection of toxic metal ions based on the LSPR band of the Au NRs and the types of interactions between the surface of Au NRs and metal ions. We summarize the work that has been done on Au NR-based longitudinal LSPR detection of environmentally toxic metal ions, sensing mechanisms, and the current progress in various modified Au NR-based longitudinal LSPR sensors for toxic metal ions. Finally, we discuss the applications of Au NR-based longitudinal LSPR sensors to real sample analysis and some of the future challenges facing longitudinal LSPR-based sensors for the detection of toxic metal ions toward commercial devices.

Received 18th December 2014,

Accepted 18th February 2015

DOI: 10.1039/c4an02330g

www.rsc.org/analyst

1. Introduction

Gold nanorods (Au NRs) are elongated nanoparticles with unique optical properties, which depend on their size and aspect ratio (their length-to-breadth ratio).^{1–7} Au NRs possess two principal plasmon absorption bands: a transverse localized surface plasmon resonance (transverse LSPR) band located in the visible region around 520 nm and a longitudinal localized surface plasmon resonance (longitudinal LSPR) band located in a longer wavelength region which can be tuned by varying the aspect ratio of the Au NRs from the visible to the near-IR region.^{1–9} The unique properties of Au NRs find applications in the fields of imaging, therapy and sensing.^{9–12} A

sensor is a device that measures or detects a physical parameter and converts it into a signal, which is subsequently read by an observer or instrument.¹³ Fig. 1 shows a schematic representation of three main components of a sensor system, the analyte (target sample), the transducer (platform/probe), and the signal-processing device.¹⁴ An optical sensor involves the addition of the target analyte of our interest to a sensor probe or transducer, which gives a detectable signal providing the analyte information.¹⁵ Optical sensors have several advantages compared to other sensing methods, such as unmatched sensitivity, multianalyte detection, non-invasiveness, and low toxicity.¹⁶ Optical sensor research is mainly driven by the needs of clinical chemistry, biotechnology and environmental chemistry.^{14,16}

In recent years, the development of new materials is essential for the advancement of optical sensors. The nanomaterial-based optical sensors have extensive applications with improved sensitivity, and selectivity, lower production costs, reduced power consumption and improved stability.¹⁷ The unique optical properties of nanoscale materials make them ideal candidates for new generation sensing devices for optical sensor applications.¹⁸ An efficient sensor has a better response time, signal-to-noise (S/N) ratio, selectivity, and limit of detection.

^aLow Dimensional Materials Research Centre, Department of Physics, Faculty of Science, University of Malaya, 50603 Kuala Lumpur, Malaysia.

E-mail: jayabal84@gmail.com, huangnayming@um.edu.my

^bDepartment of Chemistry, Faculty of Science & Functional Device Laboratory, Institute of Advanced Technology, Universiti Putra Malaysia, 43400 UPM Serdang, Selangor, Malaysia

^cSchool of Chemistry, Centre for Photoelectrochemistry, Madurai Kamaraj University, Madurai-625021, India

^dSchool of Engineering and Mathematical Sciences, City University London, London EC1V 0HB, UK



Fig. 1 Schematic representation of the main components of the sensor system.

tion (LOD).¹⁹ Therefore, designing an efficient sensor depends on the properties of novel materials that improve the potential sensing performance.¹⁸ Particularly, Au NRs have unique optical properties that give them great utility in the design of novel sensors for the detection of target analytes.

The most common optical sensors are absorption- and luminescence-based sensors.¹⁴ For Au NR-based longitudinal LSPR sensors, the absorption-based sensors are commonly developed by using the longitudinal LSPR band of Au NRs.^{1–3} Absorption-based colorimetric sensors have been developed based on the shift observed in the longitudinal LSPR band of Au NRs due to (i) the change in the interparticle distance of the NRs and (ii) the change in the refractive index of the local surrounding environment. Colorimetric sensors are extremely attractive because target analytes can be simply detected with the naked eye in the presence of interference.^{19,20} Colorimetric sensors based on nanomaterials have attracted much attention in recent years due to their simplicity, rapidity and novelty.^{19,21–23} Therefore, a Au NR-based longitudinal LSPR sensor is effectively used as a principle for optical detection of target analytes. For the development of selective and sensitive detection of specific target analytes, Au NRs are usually modified with functional group biomolecules or functionalized silica-based materials, which interact selectively with the target analytes of interest, making them detectable using the longitudinal LSPR band of the modified Au NRs.^{3,4}

The term toxic metal ions refers to metallic elements that have a relatively high density and are poisonous even at low concentrations.²⁴ The toxic metal ions are not biodegradable, hence they commonly exist in air, water and soil.^{13,20,25–32} For this reason, safety limits or maximum levels for the toxic

metal ions present in drinking water have been fixed by World Health Organization (WHO) and Environmental Protection Agency (EPA) from all over the world.³³ The toxic metal ions have a tendency to form complexes with biological ligands containing nitrogen, sulfur, and oxygen which produces changes in the molecular structure of proteins, resulting in the breaking of hydrogen bonds or inhibition of enzymes.^{25–32} These interactions may lead to toxicological and carcinogenic effects. In particular, the metal ions such as Hg^{2+} , Pb^{2+} , and As^{3+} ions affect the central nervous system; Cu^{2+} , Cd^{2+} , Hg^{2+} , and Pb^{2+} ions affect the kidneys and liver; and Ni^{2+} , Cu^{2+} , Cd^{2+} , and Cr^{3+} ions affect the skin, bones, and teeth.^{25–32} Therefore, the development of simple methods to detect traces of toxic metal ions in environmental and living systems is extremely relevant for controlling the pollution of metal ions. In recent years, the Au NRs have been used for the detection of metal ions by utilizing their longitudinal LSPR/interparticle distance dependent optical properties and high extinction coefficients.^{34,35}

In this review article, we summarize the use of a surface-modified Au NR-based longitudinal LSPR sensor as an effective platform for the detection of metal ions and also discuss different surface modification methods for Au NRs, Au NR-based longitudinal LSPR detection methods, and different interactions between the surface of the NRs and metal ions. Finally, we discuss the practical applications to real sample analysis and some key future challenges to improve the sensitivity and selectivity of the proposed sensor. We hope and expect that this review will be useful to newcomers and give direction in the field of Au NR-based longitudinal LSPR sensors.



Subramaniam Jayabal

Subramaniam Jayabal received his M.Sc. (2007) and M.Phil. (2008) degrees in Chemistry from Madurai Kamaraj University. In 2014, he submitted his Ph.D thesis in chemistry to Madurai Kamaraj University under the supervision of Prof. R. Ramaraj. Currently, he is working with Dr Nay Ming Huang as a Research Assistant at the University of Malaya. His research interest focuses on the synthesis of nanostructured materials for catalysis, sensor, and energy applications.



Alagarsamy Pandikumar

Alagarsamy Pandikumar received his B.Sc. and M.Sc. degrees from Gandhigram Rural University in 2004 and 2006, respectively. He received his Ph.D. degree (2014) in Chemistry from Madurai Kamaraj University. Currently, he is working as a HIR-Post Doctoral Research Fellow at the University of Malaya. His current research interests include graphene-based metal and metal oxide nanocomposites for photocatalysis, photoelectrochemical cells, dye-sensitized solar cells, and sensor applications.

2. Properties of Au NRs

The optical properties of metallic NPs usually arise from localized surface plasmon resonance, which occurs when the incoming electromagnetic radiation interacts with the conduction band free electrons. This induces the coherent oscillation of free electrons, which gives rise to a strong absorption band in the visible-NIR region of the electromagnetic spectrum depending on the size and shape of the particles, and also shows remarkable bright colors which could not be observed in the bulk materials.^{36–39} When spherical Au NPs are exposed to incoming electromagnetic radiation, the free electrons present in the conduction band are excited, and the columbic electrostatic attraction of the nuclei will restore these free electrons to their original positions, resulting in coherent oscillations of the free electrons when the frequency of the light oscillations matches that of the incident light (Fig. 2).^{36–39} The position of the SPR band strongly depends on the size and shape of the nanoparticles. When the shape of the nanoparticles changes, the surface geometry also changes, with a shift in the local electric field density on the particle surface upon the irradiation of light, which finally causes a change in the frequency of the oscillations.³⁶ In particular, for Au NRs, the SPR absorption splits into two bands corresponding to the oscillation of the free electrons along (longitudinal mode) and perpendicular (transverse mode) to the long axis of the NRs (Fig. 2). The transverse LSPR band (transverse mode) shows absorption at around 520 nm, while the longitudinal LSPR band (longitudinal mode) usually shows absorption at a longer wavelength and strongly depends on the aspect ratio of the NRs (Fig. 3).^{1–3} If the aspect ratio of the Au NRs is increased, the wavelength of the longitudinal LSPR band is shifted to a longer wavelength and the color of the NR solution also changes.⁴⁰

The presence of the longitudinal LSPR band in Au NRs is extremely sensitive to any change in the refractive index of the

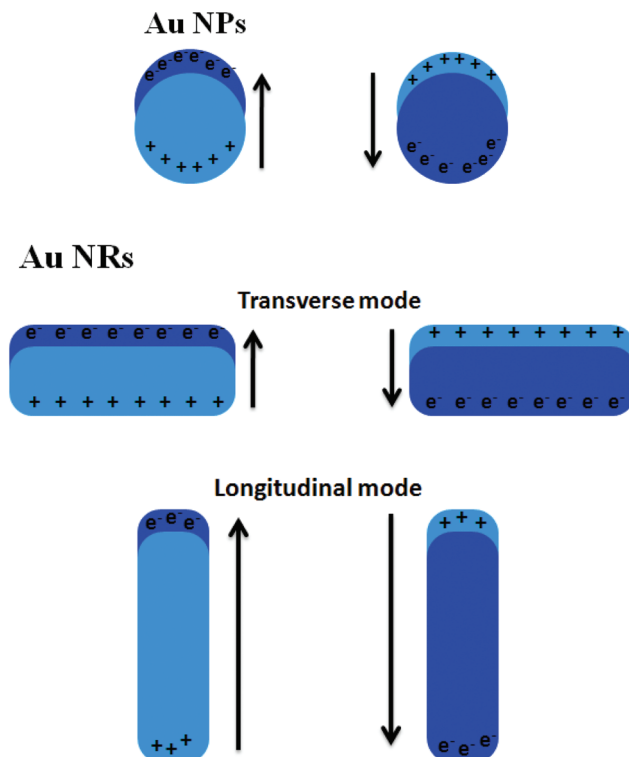
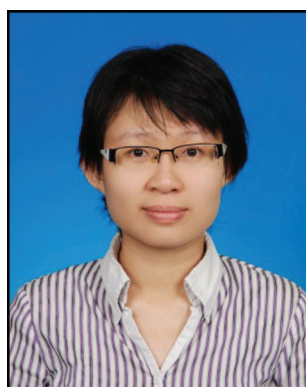


Fig. 2 Schematic representation of SPR excitation for Au NPs and Au NRs.

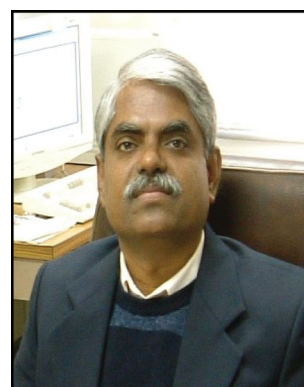
solvent and the presence of a capping agent or shell layer on the surface of the NRs.¹ The excellent sensitivity of the longitudinal LSPR band is also due to the interparticle distance between the Au NRs. The presence of a strong longitudinal LSPR absorption intensity in Au NRs gives rise to improved sensitivity in the field of optical sensors.^{3,34} Therefore, the longitudinal LSPR band is very sensitive to the local surround-



Hong Ngee Lim

Senior Lecturer. Since 2009, she has been actively involved in graphene-related research, encompassing the synthesis of graphene-based nanomaterials and their applications.

Hong Ngee Lim received her B.Sc. and M.Sc. degrees from the Universiti Kebangsaan Malaysia in 2002 and 2004, respectively. She was awarded a Ph.D. degree in Chemistry from the Universiti Putra Malaysia in 2010. Her research experience involves working as an Assistant Professor at the Nottingham University Malaysia Campus and as a Senior Lecturer in the University of Malaya before joining the Universiti Putra Malaysia as a



Ramasamy Ramaraj

he is extensively working on nanomaterial-modified electrodes and photoelectrocatalysis. He is currently a visiting professor at the University of Malaya.

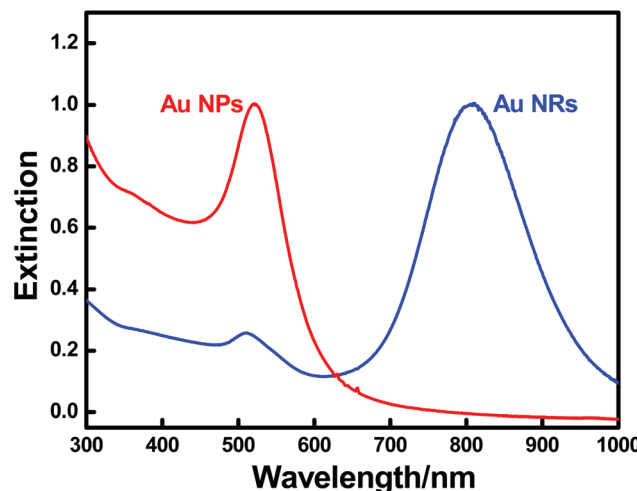


Fig. 3 Normalized extinction spectra of spherical Au NPs and Au NRs.

ing environment, when compared to the transverse LSPR band, as well as the SPR band of spherical Au NPs. This is due to the presence of the following two effects:

- (i) Strong light scattering and
- (ii) Large electric field enhancement

The longitudinal LSPR band strongly depends on the scattering and absorption of light, along with the electric field intensity at the surface of the NRs.^{1–3} The scattering and absorption components strongly depend on the surface properties of Au NRs.^{1–3,41,42} The position of the longitudinal LSPR band is easily measured using a conventional UV-visible spectrophotometer and it appears as a band at longer wavelengths (600–1100 nm), which depends on the aspect ratio of the NRs. The Au NRs scatter light very efficiently compared to spherical Au NPs, and are also involved in the measurement of the UV-visible spectrum (extinction spectrum).⁴³ The extinc-

tion spectrum is the combination of absorption and scattering.^{44,45} The enhancement of the electric field is due to the surface plasmon oscillations generated with the incoming light.^{3,36} The local electric field density strongly depends on the geometry of the metallic NPs.^{3,36} For Au NRs, the high intensity of the longitudinal LSPR band is due to strong surface plasmon oscillations in longitudinal mode compared to the surface plasmon oscillations of the transverse LSPR band and spherical Au NPs, which leads to a large enhancement of the electric field at the NR surface.^{3,46,47} In particular, Au NRs have a higher electric field generated at the tips and edges of the NRs.^{3,46,47} Because of the presence of a strong scattering effect and large electric field enhancement upon the irradiation of light, Au NRs can be effectively used in applications in the fields of chemical sensors, surface-enhanced Raman scattering (SERS), and biological imaging.^{1,3,9}

3. Preparation of Au NRs

The preparation of Au NRs with a high yield and uniform shape control is necessary to ensure their unique optical properties for various applications. The preparation of Au NRs with a 100% yield of NRs is a difficult task.⁴⁸ Therefore, the preparation of Au NRs with a higher yield and uniform shape has been an emerging field in recent years. For the preparation of Au NRs, there are two general methods, *i.e.* bottom-up and top-down methods.³ In the bottom-up methods, Au NRs are prepared by the growth of particles starting from metal atoms, which are obtained from Au precursors. These include the wet chemical method,^{48–52} electrochemical method,⁵³ sonochemical method,⁵⁴ photochemical method,⁵⁵ solvothermal method,⁵⁶ and microwave-assisted method.⁵⁷ In these methods, Au NRs are prepared by the reduction of Au salts using various reducing agents such as sodium borohydride,



Tong Sun

Tong Sun was awarded the degrees of Bachelor of Engineering, Master of Engineering and Doctor of Engineering at the Department of Precision Instrumentation of the Harbin Institute of Technology, Harbin, China in 1990, 1993 and 1998 respectively. Subsequently she was promoted to a Senior Lecturer in 2003, a Reader in 2006 and a Professor in 2008 at City University, London. Tong Sun is currently leading a research

team focused on developing a range of optical fibre sensors for a variety of industrial applications, including structural condition monitoring, early fire detection, homeland security, process monitoring, food quality and environmental monitoring.



Nay Ming Huang

Nay Ming Huang received his B.Sc., M.Sc., and Ph.D. degrees from the Universiti Kebangsaan Malaysia. He joined the University of Malaya in 2009 as a Senior Lecturer in the Department of Physics, Faculty of Science. His current research interests involve graphene and graphene based nanocomposites for sensor, solar energy conversion, and energy storage applications. He was awarded the National Young Scientist award, MASS Young Scientist award and UM Young Researcher award in 2012. He has extensively worked on graphene-related research work over the past few years.

ascorbic acid, and small Au clusters, in the presence of different external agents. In the top-down methods, Au NRs are prepared by a combination of different physical lithography techniques and deposition of Au.^{3,58,59} However, the top-down methods are generally time consuming and highly expensive.³ The preparation of Au NRs by various methods and their growth mechanisms have already been discussed in many reviews by different groups such as Huang *et al.*,¹ Perez-Juste *et al.*,² Chen *et al.*,³ and Vigderman *et al.*³⁴

The most common method used for the preparation of Au NRs is the seed-mediated growth method developed by El-Sayed *et al.*⁴⁸ and Murphy *et al.*⁴⁹ because of its simplicity, high NR yield, uniform size control, and easy surface modification. In the typical seed-mediated growth method developed by El-Sayed *et al.*,⁴⁸ a seed solution of Au nanoparticles with a size of <4 nm is initially prepared by reducing chloroauric acid with borohydride in an aqueous cetyltrimethylammonium bromide (CTAB) solution. Then, the growth solution is obtained by the reduction of Au^{3+} ions into Au^+ ions with the aid of a mild reducing agent (ascorbic acid) in an aqueous CTAB solution containing AgNO_3 . Finally, a certain amount of the seed solution is added to the growth solution for the formation of Au NRs. The aspect ratio of Au NRs is controlled by varying the amount of AgNO_3 . The NR yield using this method is >99%. Here, the CTA-Br- Ag^+ complex acts as a face-specific capping agent that selectively binds with the higher-energy (110) facets of the Au nanocrystals, which slows down the growth on these facets. Thus, Au atoms will be mainly deposited onto the (100) facets, which leads to the longitudinal growth of the NR-like shape.^{3,51} Using this seed-mediated growth method in the presence of Ag^+ ions gives a single-crystalline Au NR structure.⁶⁰ Murphy *et al.*⁴⁹ prepared Au NRs by the seed-mediated growth method in the absence of Ag^+ ions. In the absence of Ag^+ ions, the prepared Au NR solution contains a mixture of rods, spheres, and plates, and the pure NRs are finally separated using centrifugation. Using this seed-mediated growth method in the absence of Ag^+ ions gives a pentahedrally twinned Au NR structure.⁶⁰ In recent years, many researchers have focused on the synthesis of Au NRs using different methods with high yields and uniformity.

4. Chemical modification of Au NRs

The direct use of Au NRs for sensors has not been widely pursued because of the CTAB bilayers capped on the surface of the Au NRs which limit the applications in the fields of nanotechnology and biology.^{2,3,7,61} The large amount of CTAB dispersed in a Au NR solution will interfere with some biomolecules and also has significant cytotoxicity.^{61–63} The unbound CTAB layers present in the Au NR solution are toxic to the cultivated cells.⁶¹ Therefore, the excess CTAB present in the Au NR solution is removed by centrifugation. After centrifugation, the obtained Au NRs are unstable, mainly because of the desorption of CTAB molecules from the Au NR surface.^{7,62,64} Therefore, the surface of the Au NRs should be

modified with specific functional group biomolecules or polymer-based materials to enhance the applications of Au NRs in the fields of nanotechnology and biology.^{65–73} The surface functionalization of Au NRs will provide a stable platform for an optical sensor system with improved sensitivity and selectivity. For the effective detection of metal ions with more advantages, the Au NRs are generally modified with a specific functionalized group that interacts selectively with the target analytes of analytical interest. The surface functionalization of Au NRs by suitable functional groups has attracted considerable attention because of the improved stability, functionality, and application potential.^{68,69} In recent years, surface modified Au NRs have constituted an emerging field, and modified Au NRs have been used for optical sensor and biological applications.^{3,9,34}

The modification of Au NRs is done by two approaches: non-covalent interactions, involving the physical adsorption of the functional groups on the surface of NRs, and covalent interactions, involving chemical binding of the functional groups on the surface of the NRs.^{74–77} The surface of the Au NRs is generally modified using different methods, which include ligand exchange, layer-by-layer (LbL), and surface coating (Table 1).^{40,69,72} Fig. 4 shows a schematic representation of the different methods for the modification of Au NRs. In the ligand exchange method, biomolecules or thiol compounds are used to modify the CTAB bilayer, which form a

Table 1 Summary of different surface modification methods

Different modification methods	Surface modifying molecules/compounds/materials	Ref.
Ligand exchange	Biomolecules and thiol compounds.	78,79
Layer-by-layer (LbL)	Anionic and cationic polyelectrolytes	80,81
Surface coating	Polymer and silica materials	86,87

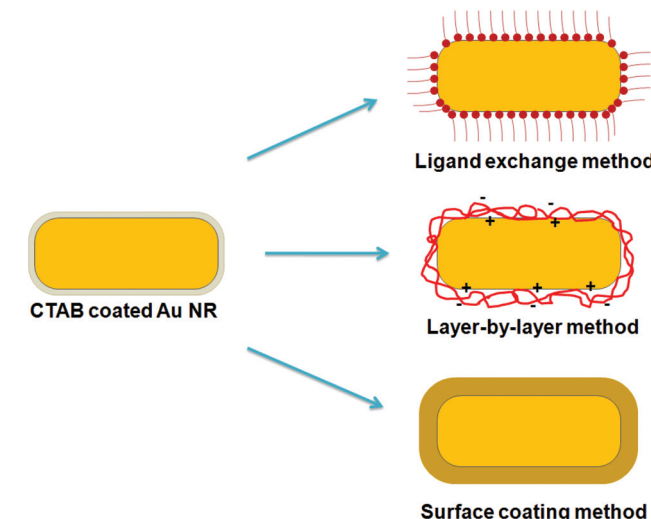


Fig. 4 Schematic representation of different methods for modification of Au NRs.

strong bond with the surface of the Au NRs.^{78,79} Takahashi *et al.*⁷⁸ reported a method for the preparation of modified Au NRs using phosphatidylcholine, which reduces the cytotoxicity of the Au NRs for practical applications. Dai *et al.*⁷⁹ developed a method for the efficient replacement of the CTAB bilayer surfactants on Au NRs using the bifunctional thiol ligand 11-mercaptoundecanoic acid inside an ionic exchange resin, which resulted in good solubility and stability against the aggregation of Au NRs in organic solvents. Layer-by-layer (LbL) approaches involve the effective coating of the NR surface without removing the CTAB bilayer. The LbL approach involves the sequential deposition of anionic and cationic polyelectrolytes with oppositely charged surfaces through electrostatic self-assembly.⁶⁹ The first step involves the adsorption of an anionic polyelectrolyte due to the presence of the cationic surfactant CTAB on the surface of the Au NRs. Gole *et al.*⁸⁰ reported a method for the preparation of polyelectrolyte-coated Au NRs by the LbL technique using poly(sodium-4-styrenesulfonate) and poly(diallyldimethylammonium chloride) as electrolytes. Takahashi *et al.*⁸¹ also developed a method for the preparation of modified Au NRs with bovine serum albumin and polyethylenimine by using the LbL technique and showed cellular uptake activity. Although this method makes it simple to prepare a uniform coating thickness using cationic and anionic polyelectrolytes, the bonding between the polymer and the surface of the Au NRs is noncovalent, which leads to low stability, and the polyelectrolytes limit the surface functionality of the Au NRs.⁸² Surface coating of Au NRs by silica- or polymer-based materials reduces their interparticle aggregation and thereby enhances their stability.² In addition, the silica-based surface-coated Au NRs possess a large pore size, high surface area, good stability, and biocompatibility.^{83–85} When compared to other modification methods, silica-based modified Au NRs have been widely used because of the simple modification process and have demonstrated effective applications in sensor fields. Sendroiu *et al.*⁸⁶ reported a method for coating a thin shell of silica over Au NRs using 3-mercaptopropyl trimethoxysilane and sodium silicate for the functionalization of amine modified single-stranded DNA to improve the sensitivity of surface plasmon resonance imaging measurements on DNA microarrays. Wang *et al.*⁸⁷ prepared mesoporous silica-coated Au NRs using tetraethoxysilane in a NaOH medium for the sensitive colorimetric detection of ascorbic acid induced by silver overcoating.

The surface modified Au NRs showed a significant change in the wavelength of the longitudinal LSPR band, along with a small change in the transverse LSPR band of the Au NRs. These changes are due to the (i) change in the local refractive index of the medium surrounding the NRs after modification and (ii) the change in the aspect ratio of the NRs after modification.^{83,88} The surface functionalized Au NRs will act both as a recognition element for the analyte receptor and a transducer for signal processing, thereby simplifying the sensor design, with improved sensitivity and selectivity. Fig. 5 shows a pictorial diagram of the various applications of surface-modified Au NRs.^{9,11,12,87,89}

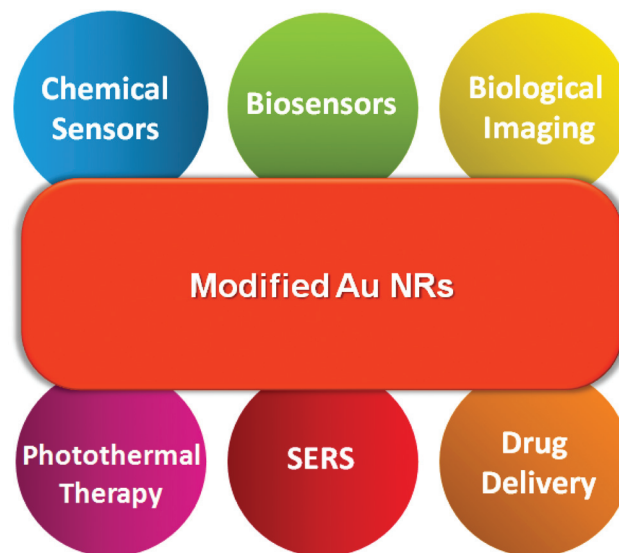


Fig. 5 Pictorial diagram of various applications of surface-modified Au NRs.

5. Au NR-based LSPR detection of metal ions

5.1. Different detection methods

5.1.1. Absorption-based detection. UV-visible (absorption)-based sensing has generally been used for the detection of toxic metal ions using Au NR-based probes. The absorption-based sensor mechanism is the measurement of the shift in the wavelength of the longitudinal LSPR band during the interaction of metal ions with the surface of a Au NR probe due to the change in the dielectric constant of the surrounding medium and also changes in the interparticle distance of the NRs after formation of the assembly or aggregation.^{3,34} This type of absorption-based detection method using Au NRs for the sensing of metal ions exhibits a much higher sensitivity than spherical Au NPs.⁹⁰

The surface modified Au NR-based sensor systems show good sensitivity and selectivity toward the target analytes.^{87,90} The Au NRs chemically modified with a specific functional group will preconcentrate the target analytes around the surface of the NRs and produce an effective adsorption of analytes on the surface of the Au NRs. Fig. 6 shows a schematic representation of an absorption-based detection system using modified Au NR probes. The interaction between the surface modified Au NRs and target analytes alters the physicochemical properties of the transducer Au NRs, such as the longitudinal LSPR absorption, scattering, and local electric field density. Finally these changes produce a detectable response signal. The interaction of metal ions with the surface of modified Au NRs will change the dielectric constant of the surrounding material, which induces changes in the frequency of the oscillation due to the change in the electron density on the surface of the NRs. As a result, a considerable shift is observed in the longitudinal LSPR absorption band of the Au NRs. The

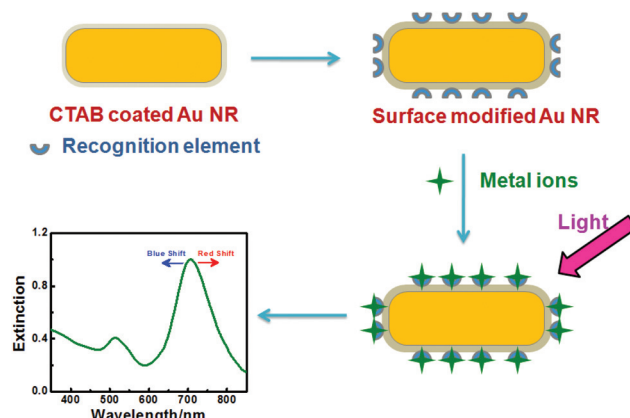


Fig. 6 Schematic representation of the absorption-based detection system using modified Au NRs.

shift in the wavelength of the longitudinal LSPR absorption band to a shorter or longer wavelength depends upon the type of the interaction of the metal ions with the surface of the Au NR probe, as discussed in later sub-sections. Therefore, a Au NR-based probe/transducer is used as an effective platform for the selective and sensitive detection of toxic metal ions. The absorption-based detection of various metal ions using Au NR-based probes is tabulated in Table 2.

The absorption-based colorimetric detection method has attracted great interest because of their unique advantages

such as simplicity, novelty, low cost and lack of analytical instrumentation requirements.^{21,22,91–95} The colorimetric detection of metal ions using Au NR-based systems is a proof-of-concept for the development of a sensor system, since it is easily visible to the naked eye in the detection of Hg^{2+} ions with high sensitivity and selectivity. The color of the Au NRs depends on their aspect ratio and the dielectric constant of the surrounding medium, which includes the stabilizing agent, functionalization, and shell coating on the surface of the NRs.^{1–3} By using the color dependent properties, Au NR-based sensor systems can be effectively used for colorimetric detection of toxic metal ions. The color change during the aggregation (or assembly or morphology change) of Au NR-based probes provides a convenient analytical platform for the absorption-based colorimetric detection of any specific target analyte. The aggregation of the Au NRs produces a decrease in the interparticle distance of the NRs, which results in changes in the plasmon coupling and leads to a color change, even at very low concentrations.¹⁸ The sensitivity and selectivity of Au NR-based sensors depend on their aspect ratio and density of NRs, as well as the nature of the target analytes.

Placido *et al.*⁹⁶ reported colorimetric sensing of Hg^{2+} ions using pyrazole-derived amino ligand functionalized Au NRs. Upon the addition of 30 ppb Hg^{2+} ions, the color of the solution is changed with a red shift in the longitudinal LSPR band of the Au NR probes, as shown in Fig. 7.

Table 2 Summary of reports in the literature on Au NR-based probes for metal ion sensing

Probe	Detection method	Metal ions	Type of interaction	Linear range	LOD	Ref.
PyL-Au NRs	Absorption and colorimetric	Hg^{2+}	End-to-end assembly formation	0–6 ppb	11 pM (3 ppt)	96
TPDT silicate-Au NRs	Absorption and colorimetric	Hg^{2+}	Morphology change and AuHg amalgamation	1 μ M–7 μ M	0.317 μ M	97
Au NRs	Absorption	Fe^{2+}	End-to-end assembly formation	—	—	113
Cys-Au NRs	Absorption and colorimetric	Cu^{2+}	End-to-end assembly formation	1–100 μ M	0.34 μ M	114
Cys-Au NRs	Absorption	Pb^{2+}	Side-by-side assembly and aggregation	0.1 nM–1 nM	0.1 nM	115
DTT-Au NRs	Absorption	Hg^{2+}	Aggregation	1–50 nM	0.42 nM	116
ssDNA-Au NRs	Absorption and colorimetric	Pb^{2+}	Aggregation	5 nM–1 μ M	3 nM	117
Au NRs	Absorption	Hg^{2+}	AuHg amalgam formation and morphology changes	1.98×10^{-12} – $3.11 \times 10^{-8} \text{ g L}^{-1}$	$2.43 \text{ fM (6.6} \times 10^{-13} \text{ g L}^{-1})$	118
Au NRs	Absorption	Hg^{2+}	AuHg amalgam formation and morphology changes	$2.0 \mu\text{g L}^{-1}$ – 0.58 mg L^{-1}	$3.68 \text{ nM (1 } \mu\text{g L}^{-1})$	119
Silica-CN-Au NRs	Colorimetric	Hg^{2+}	AuHg amalgam formation	50 nM–5 μ M	5.4 nM	120
Au NRs	Absorption	Hg^{2+}	AuHg amalgam formation	—	—	121
Au NRs	Absorption and colorimetric	Cu^{2+}	Catalytic etching	5 nM–500 mM	1.6 nM	122
Au NRs	Colorimetric	Cu^{2+}	Catalytic etching	10–300 nM	4.96 nM	123
Au NRs	Colorimetric	Pb^{2+}	Etching and Pd–Au alloy formation	10 nM–1 μ M	4.3 nM	124
Au NRs	Colorimetric	Cu^{2+}	Catalytic etching	7–50 nM	2.7 nM	125
Au NRs	Absorption	Fe^{3+}	Agglomeration	—	0.25 μ M (100 ppb)	126
MS-Au NRs	Absorption and colorimetric	Hg^{2+}	Redox-mediated inner particle interaction	1 nM–1 mM	0.79 nM	90
Polyamine-capped Au NRs	Absorption	Cu^{2+}	Chelation	1 μ M–5 mM	0.24 μ M	127
Au NRs	Absorption	Fe^{3+} , Hg^{2+} , Cu^{2+} , and Ag^{+}	Changes of the nanostructure and composition	—	—	128

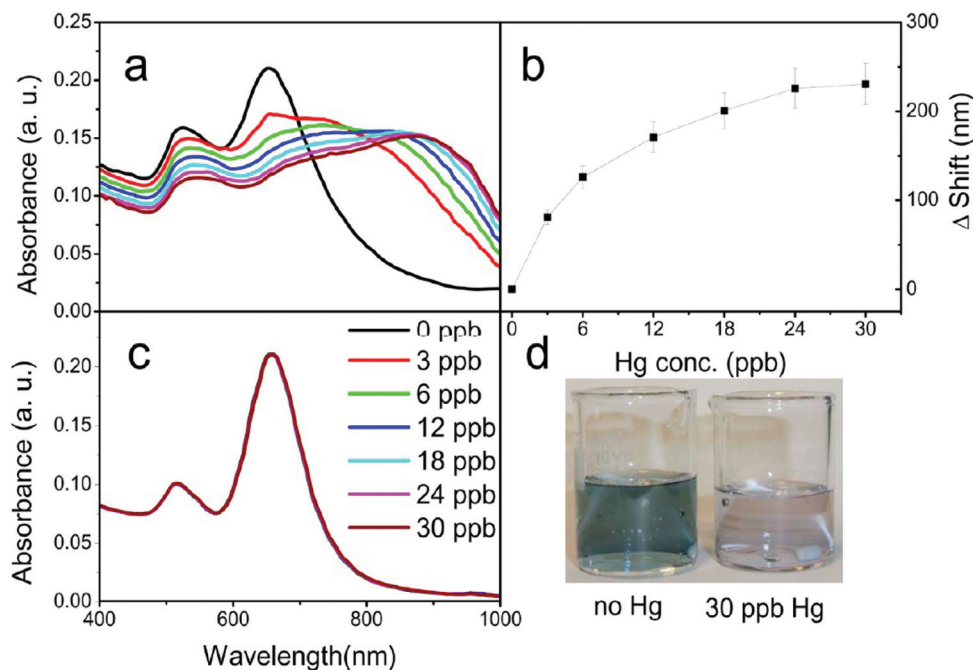


Fig. 7 UV–vis absorption spectra of (a) “PyL treated” Au NRs upon addition of increasing concentrations of Hg^{2+} ions (from 0 to 30 ppb), (b) shift in the longitudinal LSPR band with increasing concentrations of Hg^{2+} ions, (c) “as prepared” Au NRs with increasing concentrations of Hg^{2+} ions, and (d) photograph of beakers containing a Au NR solution before and after addition of Hg^{2+} ions. Reproduced with permission from ref. 96 Copyright 2013 The American Chemical Society.

In an another study, Jayabal *et al.*⁹⁷ developed a selective colorimetric sensor for the detection of Hg^{2+} ions using Au NRs embedded in a silicate sol-gel matrix. The longitudinal LSPR absorption band of the Au NRs in the silicate sol-gel showed a blue shift with a significant decrease in the absorption intensity upon 1 μM increases in the concentration of Hg^{2+} ions. Fig. 8 presents a plot of the shift in the LSPR band maximum (λ_{LSPR}) of the Au NRs in the silicate sol-gel against the concentration of Hg^{2+} ions, which shows two linear lines corresponding to the lower (1 μM to 10 μM) and higher (10 μM to 20 μM) concentrations of Hg^{2+} ions. The addition of 10 μM concentration of Hg^{2+} ions to the Au NRs in the silicate sol-gel

solution led to a color change, and this trend correlates with the two linear lines at the lower and higher concentrations observed in the plot (Fig. 8). The colorimetric sensing of various metal ions using Au NR-based probes is tabulated in Table 2.

5.1.2. Other detection methods. There are various methods reported for the detection of toxic metal ions using Au NRs as a probe, including fluorescence resonance energy transfer (FRET),^{98,99} plasmon resonance energy transfer (PRET),¹⁰⁰ plasmonic circular dichroism,¹⁰¹ and surface-enhanced Raman scattering (SERS)¹⁰² techniques and the standard techniques for the detection of trace metal ions such as atomic absorption spectroscopy¹⁰³ (AAS), inductively

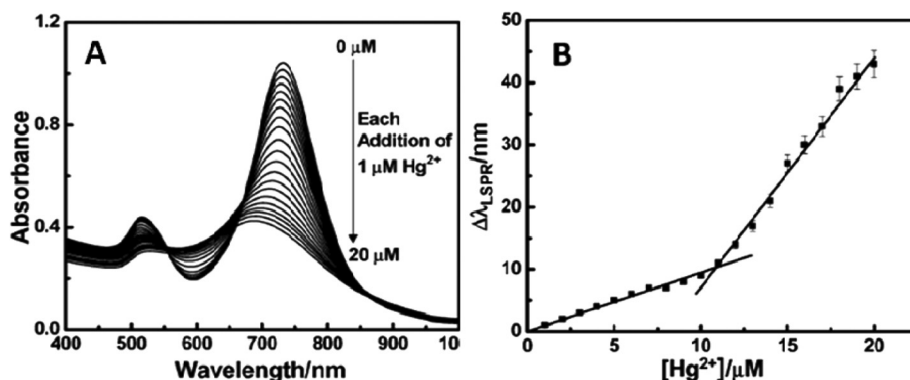


Fig. 8 (A) Absorption spectral changes observed for Au–TPDT NRs upon each 1 μM addition of Hg^{2+} ions to the solution. (B) Plot of the shift in the longitudinal LSPR band maximum ($\Delta\lambda_{\text{LSPR}}$) of Au–TPDT NRs against concentrations of Hg^{2+} ions. Reproduced with permission from ref. 97 Copyright 2014 The Royal Society of Chemistry.

coupled plasma-mass spectrometry¹⁰⁴ (ICP-MS), and electrochemical¹⁰⁵ methods. Although these techniques offer sufficient sensitivity towards the detection of toxic metal ions, each method has its own advantages and drawbacks. Moreover, these methods are time-consuming, require complex instrumentation, trained professionals, and complicated sample preparation processes. The Au NR-based longitudinal LSPR sensor provides simplicity, a short time delay, cost-effectiveness, good selectivity and sensitivity. Hence, the detection of toxic metal ions using the Au NR-based longitudinal LSPR method is more suitable sensor platform for evaluating low concentrations of toxic metal ions.

5.2. Interactions involved in the detection of metal ions using Au NRs

The Au NRs prepared by a seed-mediated growth method in the absence of Ag⁺ ions have a five-fold twinned NR structure, and in the presence of Ag⁺ ions, a single-crystalline NR structure is obtained.^{48,49,60} The five-fold twinned Au NRs have a side-facet of (110) and an edge-facet of (111), and single-crystalline NRs have side-facets of (110) or (100) and edge-facets of (111) or (100), which depend on the cross-sections of the NRs.^{106,107} The surface energy of the (110) crystallographic facets is higher than that of the (100) and (111) facets.^{108,109} The side facet (110) is thickly covered with a CTAB bilayer whereas the end-facets (111) and (100) are less thickly covered due to the lower surface energies of the (111) and (100) facets compared to the (110) facet. Thus, the CTAB bilayer predominately binds with the conventionally less stable (110) facet and produces more stability. The presence of side-facets (110) or (100) and edge-facets (111) or (100) is beneficial for surface modification and also induces specific interactions with the surface of the Au NRs and metal ions, whereas such a specific interaction is not possible in the Au spherical nanoparticles which consist of only (111) and (100) surface facets.¹¹⁰ Fig. 9 shows different structural models of the Au NRs, with their

specific planes. The interaction between the metal ion and the surface of the Au NR probe gives rise to various types of interactions including end-to-end assembly formation, side-by-side assembly formation, aggregation-based formation, etc.

5.2.1. End-to-end assembly formation. In the end-to-end assembly interaction, the metal ions preferentially bind with the (111) or (100) facets present in the edges of the modified Au NRs through specific interactions or binding leading to chain/wire-like formation. The end-to-end assembly formation in the Au NRs with the specific interaction of the target analytes generally causes a red shift in the longitudinal LSPR band, with no significant shift in the transverse LSPR band. A schematic representation of the end-to-end assembly formation in the sensing of metal ions using modified Au NRs is shown in Fig. 10.

The red shift observed in the longitudinal LSPR band is due to the decrease in the internanorod distance upon end-to-end assembly formation.^{98,109–111} The strength of the longitudinal plasmon coupling increases with the decreasing internanorod distance, which results in a red shift in the longitudinal LSPR band for the end-to-end assembly formation. When the number of NRs increases in this assembly formation, the strength of the longitudinal plasmon coupling also increases, which results in a larger red shift in the longitudinal LSPR band.¹¹² This inter-nanorod plasmon coupling mechanism can be qualitatively correlated with the exciton coupling theory by treating the NR plasmon oscillation as an exciton. In the exciton coupling theory,¹¹² the excited-state plasmon modes of the monomer split into either in-phase (symmetric) or out-of-phase (antisymmetric) modes, leading to the formation of a lower energy bonding plasmon mode or a higher energy antibonding plasmon mode, respectively (Fig. 11). If the incident polarization is along the longitudinal axis of the end-to-end NR dimer, the excited state plasmon mode is favored in the in-phase transition at lower energy because of the attractive dipole moments of the two NRs in the longitudinal polarization configuration, which produces a red shift in the longitudinal LSPR band. In contrast, the out-of-phase transition at a higher energy is not favored because of the cancellation of the two dipole moments in the longitudinal polarization configuration (Fig. 11). Because of the attractive dipole interaction at a lower energy, the end-to-end assembly interaction is more sensitive than the side-by-side assembly interaction.

Placido *et al.*⁹⁶ reported the preparation of pyrazole-derived amino ligand functionalized Au NRs for the detection of Hg²⁺ ions, where an increase in the concentration of the Hg²⁺ ions causes a gradual red shift and broadening of the longitudinal LSPR band due to the formation of end-to-end assembly (Fig. 7). The Hg²⁺ ions interact preferably at their tips with the specific topology of the ligand-modified Au NRs. The LOD obtained by using this method was 11 pM (3 ppt), which is lower than the EPA standard for the maximum allowable level (10 nM) of mercury in drinking water. Selvakannan *et al.*¹¹³ prepared thiol-terminated terpyridine functionalized Au NRs which selectively bound Fe²⁺ ions through end-to-end one-dimensional self-assembly formation with decreases in the

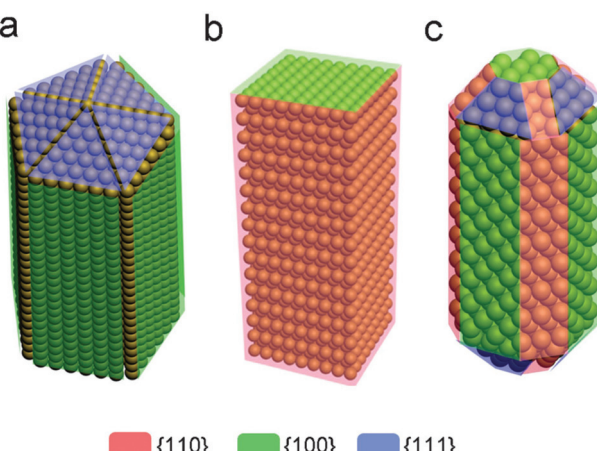


Fig. 9 Structural models of Au NRs. (a) Five-fold twinned NR, (b) single-crystalline NR with the rectangular cross-section and (c) single crystalline NR with the octagonal cross-section. Reproduced with permission from ref. 106 Copyright 2011 The Royal Society of Chemistry.

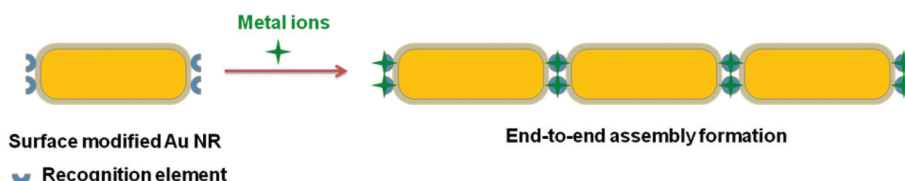


Fig. 10 Schematic representation of end-to-end assembly formation.

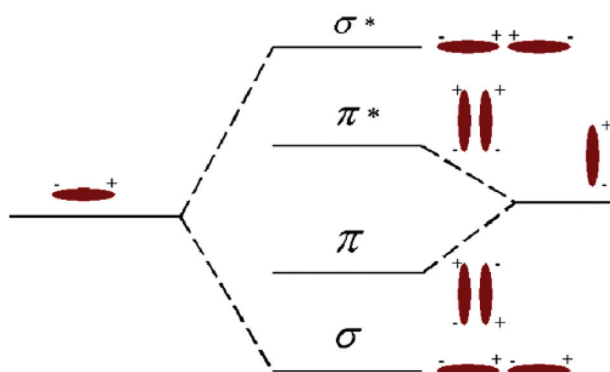


Fig. 11 Exciton theory picture of the nature of the coupled longitudinal plasmon excitation in NR dimers: electromagnetic analogy to molecular orbital theory. Reproduced with permission from ref. 112 Copyright 2006 The American Chemical Society.

intensity and a red shift in the longitudinal LSPR band due to the thiol groups binding with the (111) end facets of the NRs, which selectively bind the edges of the tips of the NRs to induce the end-to-end assembly formation. Liu *et al.*¹¹⁴ developed a probe for the selective and sensitive detection of Cu^{2+} ions using cysteine-modified Au NRs. The CTAB preferentially binds with the side faces of the Au NRs compared to the end faces and thus hinders the binding of cysteine to the side faces of the Au NRs. The detection of Cu^{2+} ions is based on the red shift in the longitudinal LSPR band due to the strong coordination of Cu^{2+} ions with cysteine, which results in a stable Cys–Cu–Cys complex through the end-to-end assembly of the Au NRs along with a color change. The LOD obtained using this method was $0.34 \mu\text{M}$, which is lower than the EPA standard for the maximum allowable level ($20 \mu\text{M}$) of copper in drinking water. This method was successfully applied to the determination of Cu^{2+} ions in tap water, lake water and river water samples.

5.2.2. Side-by-side assembly formation. In the side-by-side assembly interaction, the metal ions specifically bind with the sides of the NRs through specific interactions or binding, while the surface of the NRs is already modified with the specific functional group by utilizing the (110) side and (111) end facets present on the surface of the NRs. The assembly of Au NRs by side-by-side interactions using a specific interaction with a target analyte generally causes a blue shift in the longitudinal LSPR band and a red shift in the transverse LSPR band. A schematic representation of the side-by-side assembly interaction in the sensing of metal ions using modified Au NRs is shown in Fig. 12.

The blue shift observed in the longitudinal LSPR band is due to the decrease in the internanorod distance upon side-by-side assembly formation.^{98,112} The strength of the longitudinal plasmon coupling increases with decreasing internanorod distance, which results in a blue shift in the longitudinal LSPR band for the side-by-side assembly formation. When the number of interacting NRs increases in this assembly formation, the strength of the longitudinal plasmon coupling also increases, which results in a larger blue shift in the longitudinal LSPR band.¹¹² On the basis of the exciton coupling theory,¹¹² if the incident polarization is along the longitudinal axis of a side-by-side NR dimer (Fig. 11), the excited state plasmon mode is favored in the out-of-phase transition at higher energy because of the attractive dipole moments of the two NRs in the longitudinal polarization configuration, which produces a blue shift in the longitudinal LSPR band. In contrast, the in-phase transition at lower energy is not favored because of the cancellation of two dipole moments in the longitudinal polarization configuration. If the incident polarization is along the transverse axis of a side-by-side NR dimer (Fig. 11), the excited state plasmon mode is favored in the in-phase transition at lower energy because of the attractive dipole moments in the transverse polarization arrangement, which results in a red shift in the transverse LSPR band. In contrast, the out-of-phase transition at higher energy is not favored because of the cancellation of the two dipole moments in the transverse polarization arrangement.

Cai *et al.*¹¹⁵ prepared cysteine-functionalized Au NRs, which acted as probes for the detection of Pb^{2+} ions by the formation of side-by-side assembly interactions with a small blue shift and a decrease in the intensity of the longitudinal LSPR band along with a slight change in the transverse LSPR peak after the addition of Pb^{2+} ions. The interaction with cysteine-func-

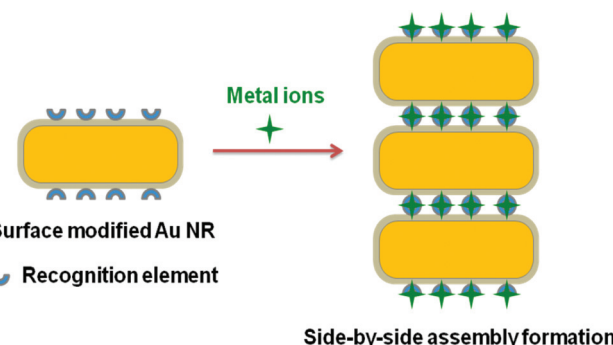


Fig. 12 Schematic representation of side-by-side assembly formation.

tionalized Au NRs involves their long sides with the Pb^{2+} ions, due to the specific topology of cysteine. The LOD obtained using this method was 0.1 nM, which is lower than the EPA standard for the maximum allowable level (75 nM) of lead in drinking water. This method was successfully applied to the determination of Pb^{2+} ions in real tap water samples.

5.2.3. Aggregation-based formation. The aggregation of Au NRs generally leads to a color change in the solution. The formation of aggregates affects the plasmonic properties of the Au NRs and also changes their absorption and scattering effects. A schematic representation of the formation of aggregates in the sensing of metal ions using modified Au NRs is shown in Fig. 13.

Bi *et al.*¹¹⁶ developed a simple method for the detection of Hg^{2+} ions using Au NRs in the presence of dithiothreitol. In

this method, Au NRs are aggregated in the presence of dithiothreitol. However, after the addition of Hg^{2+} ions, a strong coordination of Hg^{2+} ions with thiol groups present in the dithiothreitol results in a stable Hg-S bond formation with a color change and also inhibits the aggregation of the Au NRs. The LOD obtained using this method was 0.42 nM. This method was successfully applied to the determination of Hg^{2+} ions in real water samples. Chen *et al.*¹¹⁷ developed a probe for the selective and sensitive label-free colorimetric method for detection of Pb^{2+} ions using Au NRs based on the conformational switch from single-stranded DNA to a G-quadruplex. The detection of Pb^{2+} ions involves a decrease in the intensity of the longitudinal LSPR band with a blue shift due to the strong electrostatic interaction of Pb^{2+} ions with single-stranded DNA, which results in the formation of a G-quadruplex through the aggregation of the Au NRs in a side-by-side manner, along with a color change. The LOD obtained using this method was 3 nM. This method was successfully applied to the determination of Pb^{2+} ions in real tap water samples.

5.2.4. Amalgam-based formation. The amalgam-based formation sensing mechanism has attracted great interest particularly for the detection of Hg^{2+} ions. Rex *et al.*¹¹⁸ reported the use of Au NRs in the presence of an excess amount of $NaBH_4$ for the detection of Hg^{2+} ions with high sensitivity. Upon the addition of Hg^{2+} ions to the Au NR solution in the presence of excess $NaBH_4$, the morphology of the Au NRs is changed to spherical particles through an amalgamation process between the Au and Hg (Fig. 14). This is also sup-

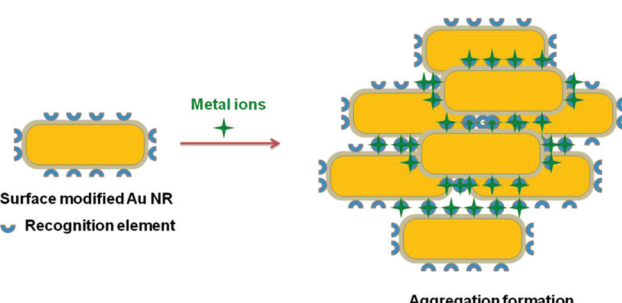


Fig. 13 Schematic representation of aggregation-based formation.

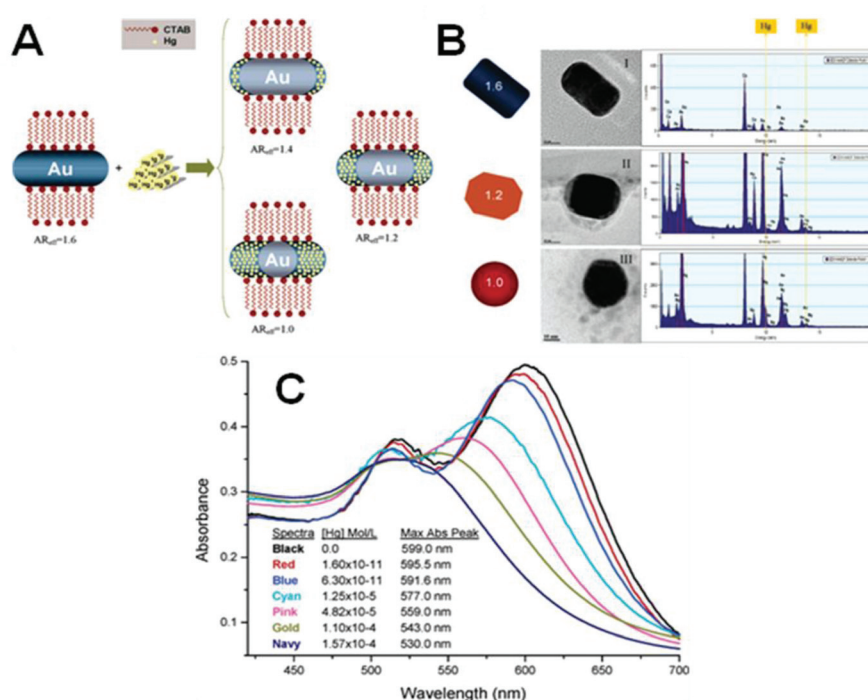


Fig. 14 (A) Schematic diagram showing amalgamation of Hg with Au NRs. (B) TEM and EDS analysis results of Au NRs in the absence of Hg^{2+} ions (I) and in the presence of Hg^{2+} ions at concentrations of 1.25×10^{-5} M (II) and 1.57×10^{-4} M (III). All solutions were prepared in 1.67×10^{-3} mol L^{-1} $NaBH_4$. (C) Absorption spectra of different concentrations of Hg^{2+} ions. Reproduced with permission from ref. 118 Copyright 2006 The American Chemical Society.

ported by the blue shift observed in the absorption spectra of the Au NRs upon each addition of Hg^{2+} ions (Fig. 14). The active sites of the Au NRs are at tips and edges, which result in the formation of amalgams more efficiently on the tips and edges of the NRs by decreasing their aspect ratio. Moreover, the shielding effect also restricts the amalgam formation of Hg on the lateral walls of the NRs, which leads to a change in the morphology of the Au NRs to spherical particles. Fig. 14(A) shows a schematic diagram of the amalgam between the Hg and Au NRs. The TEM image (Fig. 14(B)) shows that the morphology of the Au NRs is changed to spherical particles upon increasing the concentration of Hg^{2+} ions in the Au NR solution containing NaBH_4 , and the corresponding EDS analysis also shows the increasing Hg content. The LOD obtained using this method was 2.43 fM ($6.6 \times 10^{-13} \text{ g L}^{-1}$). This method was successfully applied to the determination of Hg^{2+} ions in real tap water samples.

Jayabal *et al.*⁹⁷ reported the preparation and application of an amine-functionalized silicate sol-gel matrix embedded in Au NRs for the selective detection of Hg^{2+} ions through the formation of a AuHg amalgam. Upon the addition of the Hg^{2+} ions to the amine-functionalized silicate-coated Au NRs, the Hg^{2+} ions were selectively adsorbed on the tips and edges of the NR structures, which resulted in the formation of an amalgam, with a change in the morphology of the NRs to spherical nanoparticles. Here, Au NRs were partially oxidized to Au(i) by the Hg^{2+} ions; simultaneously Hg^{2+} was reduced to $\text{Hg}(0)$, which formed a layer coating the Au NRs and led to a change in the morphology of the NR structure. The LOD obtained using this method was $0.317 \mu\text{M}$. This method was successfully applied to the determination of Hg^{2+} ions in real water samples. Chemnasiri *et al.*¹¹⁹ developed a Au NR-based mercury sensor using Au NRs on a functionalized glass substrate. The longitudinal LSPR band of the Au NRs experienced a blue shift after the addition of Hg^{2+} ions in the presence of NaBH_4 due to the formation of an amalgam. The LOD obtained using this method was 3.68 nM ($1.0 \mu\text{g L}^{-1}$). Anand *et al.*¹²⁰ developed a sensitive, selective, and label free optical method for the detection of Hg^{2+} ions using cyano ligand-functionalized Au NRs in the presence of ascorbic acid. Poly(2-aminobenzonitrile) was used for the functionalization of Au NRs. The sensing of Hg^{2+} ions is understood by the preconcentration of Hg^{2+} ions on the surface of cyano ligand-functionalized Au NRs through the interaction of the -CN groups with Hg^{2+} ions, which leads to the reduction of Hg^{2+} ions to $\text{Hg}(0)$ atoms by ascorbic acid through the formation of an amalgam. The LOD obtained using this method was 5.4 nM . This method was successfully applied to the determination of Hg^{2+} ions in tap and pond water samples. Heider *et al.*¹²¹ reported the application of thiol-functionalized Au NRs for mercury sensing with high sensitivity. The detection of Hg^{2+} ions involved changes in the longitudinal LSPR band through the formation of an AuHg amalgam in the presence of NaBH_4 . The LOD obtained using this method was $2.28 \times 10^{-19} \text{ M}$ mercury per NR. This method was successfully applied to the determination of mercury in tap water samples.

In general, the blue shift observed in the longitudinal LSPR band is due to the change in the dielectric constant of the medium surrounding the Au NRs after the coating of Hg on the surface of the Au NRs through the formation of an amalgam, and the effective aspect ratio of the NRs is also decreased upon a morphology change. The decrease in the intensity of the longitudinal LSPR band is due to the increase in the electron density of the Au NRs during the formation of the amalgam between the Au and Hg, and thereby affects the plasmonic properties of the Au NRs. When the morphology of the NRs changes, their plasmonic properties also significantly change due to the change in the surface geometry.

5.2.5. Catalytic etching. Catalytic etching is also an important sensing mechanism for the detection of toxic metal ions. Niu *et al.*¹²² developed a novel strategy for the colorimetric detection of Cu^{2+} ions using Au NRs in the presence of sodium thiosulfate and ammonia. The detection of Cu^{2+} ions involved changes in the longitudinal LSPR band by the etching of the Au NRs, which induces a decrease in their aspect ratio, and changes in the morphology of Au NRs. Moreover, this colorimetric sensor showed high sensitivity and selectivity towards the detection of Cu^{2+} ions. The LOD obtained using this method was 1.6 nM . Wang *et al.*¹²³ developed a novel method for the colorimetric detection of Cu^{2+} ions using Au NRs in the presence of H_2O_2 and thiocyanate through the decelerating etching of Au NRs. The detection of Cu^{2+} ions involves changes in the longitudinal LSPR band *via* catalytic decomposition of H_2O_2 by Cu^{2+} ions, which specifically inhibits the corrosion of Au NRs. Moreover, this method showed a sensitive and selective detection of Cu^{2+} ions without any other labeling or modification steps. The LOD obtained using this method was 4.96 nM . This method was successfully applied to the determination of Cu^{2+} ions in shellfish samples. Lan *et al.*¹²⁴ developed a simple colorimetric method for the selective detection of Pb^{2+} ions using Au NRs in the presence of thiosulfate. The detection of Pb^{2+} ions involves changes in the longitudinal LSPR band due to the etching of Au NRs through the formation of a Pd-Au alloy. The LOD obtained using this method was 4.3 nM . This method was successfully applied to the determination of Pb^{2+} ions in lake, pond, seawater, urine, and soil samples. Chen *et al.*¹²⁵ developed a colorimetric method for the sensing of Cu^{2+} ions using Au NRs in an ammonia/ammonium chloride buffer solution containing sodium thiosulfate. In this method, the longitudinal LSPR absorption intensity is decreased with a blue shift due to the etching of the Au NRs in the presence of dissolved oxygen, along with a color change from blue to light red. The LOD obtained using this method was 2.7 nM . This method was successfully applied to the determination of Cu^{2+} ions in shellfish samples.

5.2.6. Other interactions. Other than the above types of interactions, the sensing mechanism for the detection of toxic metal ions by Au NRs is also understood by the agglomeration, chemical redox-mediated inner particle interaction, chelation and changes in the structure and composition. Thatai *et al.*¹²⁶ developed a sensitive method for the detection of Fe^{3+} ions

using Au NRs as a probe. The detection of Fe^{3+} ions involved a blue shift in the longitudinal LSPR band of Au NRs through agglomeration. The LOD obtained using this method was 0.25 μM (100 ppb). Wang *et al.*⁹⁰ reported the colorimetric detection of Hg^{2+} ions using mesoporous silica-coated Au NRs based on the mechanism of chemical redox-mediated inner particle interactions. In this method, the Hg^{2+} ions are reduced to $\text{Hg}(0)$ in the presence of ascorbic acid and NaBH_4 . Then, the reduced $\text{Hg}(0)$ is deposited on the surface of the silica-coated Au NRs with a color change, and the addition of S^{2-} to this solution leads to the reverse process due to the extraction of $\text{Hg}(0)$ by S^{2-} . The LOD obtained using this method was 0.79 nM. Liu *et al.*¹²⁷ developed a probe for the selective and sensitive detection of Cu^{2+} ions using polyamine-capped Au NRs. Poly(sodium-4-styrenesulfonate) and polyethylenimine were electrostatically adsorbed on the positively charged CTAB-coated Au NRs using a layer-by-layer self-assembly method. The polyamine-capped Au NRs are employed as probes for the detection of Cu^{2+} ions. The longitudinal LSPR band of the polyamine-capped Au NRs experienced a blue shift due to the specific chelation of the polyethylenimine with Cu^{2+} ions. The LOD obtained using this method was 0.24 μM . This polyamine-capped Au NR-based LSPR sensor was successfully used for the detection of Cu^{2+} ions in river water.

Huang *et al.*¹²⁸ developed a label-free multiplex plasmonic sensor for the selective detection of different metal ions, including Fe^{3+} , Hg^{2+} , Cu^{2+} , and Ag^+ ions, based on a single type of Au NR. The detection of Fe^{3+} , Hg^{2+} , Cu^{2+} , and Ag^+ ions was based on the changes in the longitudinal LSPR band of Au NRs due to the interaction between these metal ions and Au NRs under optimized conditions, which produced changes in the nanostructure and composition of the Au NRs. The detection of Fe^{3+} , Hg^{2+} , Cu^{2+} , and Ag^+ ions and the changes in the longitudinal LSPR band of the NRs are shown in Fig. 15. This Au NR-based assay is able to successively determine all

four kinds of metal ions, along with distinguishing between them. This assay detects Fe^{3+} , Hg^{2+} , Cu^{2+} , and Ag^+ ions at as low as 10^{-6} , 10^{-8} , 10^{-10} , and 10^{-8} M concentrations, respectively.

6. Application to real sample analysis

The most important challenge for a Au NR-based sensor is its practical applications to real sample analysis. To validate the practical applicability of a developed sensor method, it should be applied to the determination of the metal ion levels in real samples. Thus, real samples were collected from different nearby sources, e.g. river water, tube well water, drinking water, and industrial effluent water. Initially, the collected water samples were filtered three times through qualitative filter paper to remove any unwanted residue. Then, the collected water samples were checked for the presence of any targeted metal ions. For the real sample analysis, a known concentration of the metal ions was added to the water samples containing the Au NR probes; the shift in the longitudinal LSPR band due to a change in the surrounding environment after the addition of the metal ions was monitored, and the corresponding shift in the longitudinal LSPR band was analyzed to determine the added metal ion content from the standard addition plot. The standard addition plot was obtained by the addition of known concentrations of metal ions to Au NR-based sensor probes.¹²⁹ By applying the standard addition method, the Au NR-based longitudinal LSPR sensor probes determined the metal ions present in the different water samples with good recovery.

Therefore, the developed Au NR-based sensor probes are a convenient means for determining the toxic metal ions present in environmental water samples. From the real sample analysis, the detection of Hg^{2+} ions did not interfere with the real water samples, which indicates that the proposed sensor has potential applications in the detection of metal ions present in real environmental samples.

7. Future challenges

Although Au NR-based longitudinal LSPR sensing is an effective platform for the detection of toxic metal ions, there are many important challenges still remaining in relation to the modification and application of such Au NR-based sensors. These include improvements in the (i) modification of Au NRs, (ii) LOD, (iii) selectivity toward one particular metal ion in the presence of other metal ions, and (iv) practical applications. The use of specific functional groups or specific biomolecules for the surface modification of Au NRs is a good example of the improvements made in the modification process and also for good stability. The LOD of the Au NR-based longitudinal LSPR sensor system can be improved by the development of modification procedures to prepare modified Au NR probes for the detection of metal ions. The surface

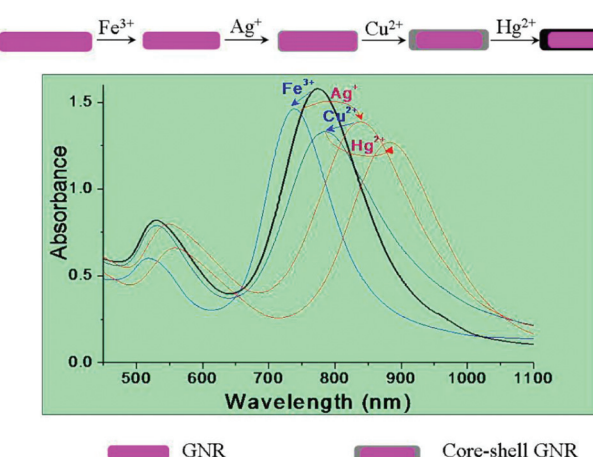


Fig. 15 Schematic illustration of determination of Fe^{3+} , Ag^+ , Cu^{2+} , and Hg^{2+} ions based on a single type of Au NR. Reproduced with permission from ref. 128 Copyright 2013 The American Chemical Society.

functionalization of Au NRs increases the surface absorption capability and fast transport of metal ions toward the surface, which enables the detection of toxic metal ions with enhanced sensitivity. The selectivity of the Au NR-based longitudinal LSPR sensor system also requires the effective modification of Au NRs using specific recognition elements as metal ion receptors. Therefore, the development of new sensor designs for the detection of toxic metal ions with more advantages such as high sensitivity, selectivity, fast response time and cost effectiveness by using modified Au NRs is the current field of interest.

Despite these challenges, clearly the unique optical properties of Au NRs and their ability to be easily modified with other materials make them ideal candidates for the detection of toxic metal ions. Au NR-based materials present a good platform for the future development of sensors to detect environmentally toxic metal ions, which could also be extended to environmentally toxic molecules. As a result, the Au NR-based LSPR sensor will be a versatile method for the detection of metal ions in the near future.

8. Conclusions

The unique optical properties of Au NRs make them an attractive platform for the detection of metal ions based on the longitudinal LSPR band of the Au NRs. The effective surface modification of Au NRs shows improved selectivity and sensitivity in the detection of toxic metal ions. Different methods are discussed for the preparation of surface-modified Au NRs for the detection of toxic metal ions based on the longitudinal LSPR band of the Au NRs, along with the types of interactions between the surface of the NRs and metal ions. In this review article, we have broadly summarized various strategies that have been implemented for the design of chemical interactions between metal ions and the surface of Au NRs. Surface functionalized Au NRs act as both recognition elements for binding with metal ions and transducers for signaling, which simplifies the design of a sensor with improved sensitivity and selectivity. The surface modification of Au NRs with functional groups will introduce a new direction in the field of sensor design. Most of the reported Au NR-based longitudinal LSPR sensors showed a lower detection limit for detection of toxic metals ions than the permissible limits of such toxic metal ions and relative to the AAS, ICP-MS, and electrochemical techniques for detection of metal ions, the Au NR-based longitudinal LSPR sensors show comparable LODs, less time consumption, and low cost instrumentation. Although the unique properties of Au NRs have offered many advantages for the detection of environmentally toxic metal ions, further efforts should be made by focusing on the development of effective modification of Au NRs to improve their stability, and specific binding with metal ions for the fabrication of sensor systems with enhanced sensitivity and selectivity. Their applications should also be extended to validate their use in real sample analysis. The chemical functionalization of Au NRs

using polymers, biomolecules, or silica-based materials allows for the fabrication of diverse range of metal ion sensors in order to improve the analytical metal ion detection performance. The Au NR-based longitudinal LSPR sensor is a versatile method for the detection of toxic metal ions.

Acknowledgements

The authors wish to express their gratitude to the Ministry of Higher Education and the University of Malaya for sanctioning a High Impact Research Grant (UM.C/625/1/HIR/MOHE/SC/21) and UMRG Programme Grant (RP007C/13AFR).

References

- X. Huang, S. Neretina and M. A. El-Sayed, *Adv. Mater.*, 2009, **21**, 4880.
- J. Perez-Juste, I. Pastoriza-Santos, L. M. Liz-Marzan and P. Mulvaney, *Coord. Chem. Rev.*, 2005, **249**, 1870.
- H. Chen, L. Shao, Q. Li and J. Wang, *Chem. Soc. Rev.*, 2013, **42**, 2679.
- T. K. Sau, A. L. Rogach, F. Jackel, T. A. Klar and J. Feldmann, *Adv. Mater.*, 2010, **22**, 1805.
- V. Sharma, K. Park and M. Srinivasarao, *Mater. Sci. Eng., R*, 2009, **65**, 1.
- J. Cao, E. K. Galbraith, T. Sun and K. T. Grattan, *Sens. Actuators, B*, 2012, **169**, 360.
- C. Wang, Z. Ma, T. Wang and Z. Su, *Adv. Funct. Mater.*, 2006, **16**, 1673.
- S. Link, M. B. Mohamed and M. A. El-Sayed, *J. Phys. Chem. B*, 1999, **103**, 3073.
- A. M. Alkilany, L. B. Thompson, S. P. Boulos, P. N. Sisco and C. J. Murphy, *Adv. Drug Delivery Rev.*, 2012, **64**, 190.
- P. K. Jain, X. Huang, I. H. El-Sayed and M. A. El-Sayed, *Acc. Chem. Res.*, 2008, **41**, 1578.
- W.-S. Kuo, C.-N. Chang, Y.-T. Chang, M.-H. Yang, Y.-H. Chien, S.-J. Chen and C.-S. Yeh, *Angew. Chem., Int. Ed.*, 2010, **49**, 2711.
- X. Huang, I. H. El-Sayed, W. Qian and M. A. El-Sayed, *J. Am. Chem. Soc.*, 2006, **128**, 2115.
- S. A. El-Safty, M. A. Shenashen and S. A. El-Safty, *Trends Anal. Chem.*, 2012, **38**, 98.
- C. McDonagh, C. S. Burke and B. D. MacCraith, *Chem. Rev.*, 2008, **108**, 400.
- N. J. Ronkainen, H. B. Halsall and W. R. Heineman, *Chem. Soc. Rev.*, 2010, **39**, 1747.
- S. Nagl and O. S. Wolfbeis, *Analyst*, 2007, **132**, 507.
- K. Kalantar-zadeh and B. Fry, *Nanotechnology-Enabled Sensors*, Springer Science+Business Media, New York, USA, 2008.
- K. Saha, S. S. Agasti, C. Kim, X. Li and V. M. Rotello, *Chem. Rev.*, 2012, **112**, 2739.
- J. Homola, *Chem. Rev.*, 2008, **108**, 462.

- 20 H. N. Kim, W. X. Ren, J. S. Kim and J. Yoon, *Chem. Soc. Rev.*, 2012, **41**, 3210.
- 21 L. Chen, X. Fu, W. Lu and L. Chen, *ACS Appl. Mater. Interfaces*, 2013, **5**, 284.
- 22 T. Lou, Z. Chen, Y. Wang and L. Chen, *ACS Appl. Mater. Interfaces*, 2011, **3**, 1568.
- 23 J. M. Slocik, J. S. Zabinski, D. M. Phillips and R. R. Naik, *Small*, 2008, **4**, 548.
- 24 J. H. Duffus, *Pure Appl. Chem.*, 2002, **74**, 793.
- 25 G. Aragay, J. Pons and A. Merkoçi, *Chem. Rev.*, 2011, **111**, 3433.
- 26 Y. Lou, Y. Zhao, J. Chen and J. J. Zhu, *J. Mater. Chem. C*, 2014, **2**, 595.
- 27 Y. W. Lin, C. C. Huang and H. T. Chang, *Analyst*, 2011, **136**, 863.
- 28 S. J. Lee, J.-E. Lee, J. Seo, Y. Jeong, S. S. Lee and J. H. Jung, *Adv. Funct. Mater.*, 2007, **17**, 3441.
- 29 S. J. Stohs and D. Bagchi, *Free Radicals Biol. Med.*, 1995, **18**, 321.
- 30 F. Fu and Q. Wang, *J. Environ. Manage.*, 2011, **92**, 407.
- 31 D. H. Nies, *Appl. Microbiol. Biotechnol.*, 1999, **51**, 730.
- 32 K. E. Giller, E. Witter and S. P. McGrath, *Soil Biol. Biochem.*, 1998, **30**, 1389.
- 33 World Health Organization, *Guidelines for drinking-water quality*, Geneva, 3rd edn, 2004, vol. 1, p. 188.
- 34 L. Vigderman, B. P. Khanal and E. R. Zubarev, *Adv. Mater.*, 2012, **24**, 4811.
- 35 T. Placido, G. Aragay, J. Pons, R. Comparelli, M. L. Curri and A. Merkoçi, *ACS Appl. Mater. Interfaces*, 2013, **5**, 1084.
- 36 S. Eustis and M. A. El-Sayed, *Chem. Soc. Rev.*, 2006, **35**, 209.
- 37 C. M. Cobley, J. Chen, E. C. Cho, L. V. Wang and Y. Xia, *Chem. Soc. Rev.*, 2011, **40**, 44.
- 38 S. K. Ghosh and T. Pal, *Chem. Rev.*, 2007, **107**, 4797.
- 39 K. G. Thomas, *Current Trends in Science*, Platinum Jubilee Special, 2009, p. 53.
- 40 L. Tong, Q. Wei, A. Wei and J. X. Cheng, *Photochem. Photobiol.*, 2009, **85**, 21.
- 41 E. Hutter and J. H. Fendler, *Adv. Mater.*, 2004, **16**, 1685.
- 42 K. A. Willets and R. P. Van Duyne, *Annu. Rev. Phys. Chem.*, 2007, **58**, 267.
- 43 C. J. Murphy, A. M. Gole, S. E. Hunyadi, J. W. Stone, P. N. Sisco, A. Alkilany and P. Hankins, *Chem. Commun.*, 2008, 544.
- 44 K. L. Kelly, E. Coronado, L. L. Zhao and G. C. Schatz, *J. Phys. Chem. B*, 2003, **107**, 668.
- 45 K. S. Lee and M. A. El-Sayed, *J. Phys. Chem. B*, 2006, **110**, 19220.
- 46 M. A. Mackey, M. R. K. Ali, L. A. Austin, R. D. Near and M. A. El-Sayed, *J. Phys. Chem. B*, 2014, **118**, 1319.
- 47 M. N'Gom, S. Li, G. Schatz, R. Erni, A. Agarwal, N. Kotov and T. B. Norris, *Phys. Rev. B: Condens. Matter*, 2008, **80**, 113411.
- 48 B. Nikoobakht and M. A. El-Sayed, *Chem. Mater.*, 2003, **15**, 1957.
- 49 N. R. Jana, L. Gearheart and C. J. Murphy, *J. Phys. Chem. B*, 2001, **105**, 4065.
- 50 A. Gole and C. J. Murphy, *Chem. Mater.*, 2004, **16**, 3633.
- 51 S. E. Lohse and C. J. Murphy, *Chem. Mater.*, 2013, **25**, 1250.
- 52 X. C. Ye, L. H. Jin, H. Caglayan, J. Chen, G. Z. Xing, C. Zheng, V. Doan-Nguyen, Y. J. Kang, N. Engheta, C. R. Kagan and C. B. Murray, *ACS Nano*, 2012, **6**, 2804.
- 53 Y.-Y. Yu, S.-S. Chang, C.-L. Lee and C. R. C. Wang, *J. Phys. Chem. B*, 1997, **101**, 6661.
- 54 K. Okitsu, K. Sharyo and R. Nishimura, *Langmuir*, 2009, **25**, 7786.
- 55 F. Kim, J. H. Song and P. D. Yang, *J. Am. Chem. Soc.*, 2002, **124**, 14316.
- 56 J. M. Cao, X. J. Ma, M. B. Zheng, J. S. Liu and H. M. Ji, *Chem. Lett.*, 2005, 730.
- 57 Y.-J. Zhu and X.-L. Hu, *Chem. Lett.*, 2003, 1140.
- 58 J.-S. Huang, V. Callegari, P. Geisler, C. Brüning, J. Kern, J. C. Prangsma, X. F. Wu, T. Feichtner, J. Ziegler, P. Weinmann, M. Kamp, A. Forchel, P. Biagioli, U. Sennhauser and B. Hecht, *Nat. Commun.*, 2010, **1**, 150.
- 59 P. B. Dayal and F. Koyama, *Appl. Phys. Lett.*, 2007, **91**, 111107.
- 60 H. Petrova, J. Perez-Juste, Z. Zhang, J. Zhang, T. Kosel and G. V. Hartland, *J. Mater. Chem.*, 2006, **16**, 3957.
- 61 A. M. Alkilany, P. K. Nagaria, C. R. Hexel, T. J. Shaw, C. J. Murphy and M. D. Wyatt, *Small*, 2009, **5**, 701.
- 62 C. Kinnear, H. Dietsch, M. J. D. Clift, C. Endes, B. Rothen-Rutishauser and A. Petri-Fink, *Angew. Chem., Int. Ed.*, 2013, **52**, 1934.
- 63 T. S. Hauck, A. A. Ghazani and W. C. W. Chan, *Small*, 2008, **4**, 153.
- 64 C. J. Murphy, L. B. Thompson, A. M. Alkilany, P. N. Sisco, S. P. Boulos, S. T. Sivapalan and J. Huang, *J. Phys. Chem. Lett.*, 2010, **1**, 2867.
- 65 C. Gui and D. Cui, *Cancer Biol. Med.*, 2012, **9**, 221.
- 66 B. Thierry, J. Ng, T. Krieg and H. J. Griesser, *Chem. Commun.*, 2009, 1724.
- 67 C. Yu, L. Varghese and J. Irudayaraj, *Langmuir*, 2007, **23**, 9114.
- 68 A. Wijaya and K. Hamad-Schifferli, *Langmuir*, 2008, **24**, 9966.
- 69 S. Y. Hwang and A. R. Tao, *Pure Appl. Chem.*, 2010, **83**, 233.
- 70 J. Cao, E. K. Galbraith, T. Sun and K. T. Grattan, *Sens. Actuators, B*, 2012, **169**, 360.
- 71 Z. Ma, H. Xia, Y. Liu, B. Liu, W. Chen and Y. Zhao, *Chin. Sci. Bull.*, 2013, **58**, 2530.
- 72 Z. Zhang, J. Wang and C. Chen, *Theranostics*, 2013, **3**, 223.
- 73 E. T. Castellana, R. C. Gamez, M. E. Gomez and D. H. Russell, *Langmuir*, 2010, **26**, 6066.
- 74 V. Biju, *Chem. Soc. Rev.*, 2014, **43**, 744.
- 75 I. Willner and B. Willner, *Nano Lett.*, 2010, **10**, 3805.
- 76 R. Mout, D. F. Moyano, S. Rana and V. M. Rotello, *Chem. Soc. Rev.*, 2012, **41**, 2539.
- 77 H. Ju, X. Zhang and J. Wang, *NanoBiosensing: Principles, Development and Application*, Springer Science+Business Media, New York, USA, 2011.

- 78 H. Takahashi, Y. Niidome, T. Niidome, K. Kaneko, H. Kawasaki and S. Yamada, *Langmuir*, 2006, **22**, 2.
- 79 Q. Dai, J. Coutts, J. Zou and Q. Huo, *Chem. Commun.*, 2008, 2858.
- 80 A. Gole and C. J. Murphy, *Chem. Mater.*, 2005, **17**, 1325.
- 81 H. Takahashi, T. Niidome, T. Kawano, S. Yamada and Y. Niidome, *J. Nanopart. Res.*, 2008, **10**, 221.
- 82 J. W. Hotchkiss, A. B. Lowe and S. G. Boyes, *Chem. Mater.*, 2007, **19**, 6.
- 83 S. Liu and M.-Y. Han, *Chem. – Asian J.*, 2010, **5**, 36.
- 84 S. Jayabal and R. Ramaraj, *Electrochim. Acta*, 2013, **88**, 51.
- 85 C. Wu and Q.-H. Xu, *Langmuir*, 2009, **25**, 9441.
- 86 I. E. Sendroiu, M. E. Warner and R. M. Corn, *Langmuir*, 2009, **25**, 11282.
- 87 G. Wang, Z. Chen and L. Chen, *Nanoscale*, 2011, **3**, 1756.
- 88 S. Jayabal, P. Viswanathan and R. Ramaraj, *RSC Adv.*, 2014, **4**, 33541.
- 89 Z. Zhang, L. Wang, J. Wang, X. Jiang, X. Li, Z. Hu, Y. Ji, X. Wu and C. Chen, *Adv. Mater.*, 2012, **24**, 1418.
- 90 G. Wang, Z. Chen, W. Wang, B. Yan and L. Chen, *Analyst*, 2011, **136**, 174.
- 91 L. Polavarapu, J. Perez-Juste, Q.-H. Xu and L. M. Liz-Marzan, *J. Mater. Chem. C*, 2014, **2**, 7460.
- 92 H. Xu, Y. Wang, X. Huang, Y. Li, H. Zhang and X. Zhong, *Analyst*, 2012, **137**, 924.
- 93 Y. Si, X. Wang, Y. Li, K. Chen, J. Wang, J. Yu, H. Wang and B. Ding, *J. Mater. Chem. A*, 2014, **2**, 645.
- 94 K. Farhadi, M. Forough, R. Molaei, S. Hajizadeh and A. Rafipour, *Sens. Actuators, B*, 2012, **161**, 880.
- 95 C.-Y. Lin, C.-J. Yu, Y.-H. Lin and W.-L. Tseng, *Anal. Chem.*, 2010, **82**, 6830.
- 96 T. Placido, G. Aragay, J. Pons, R. Comparelli, M. L. Curri and A. Merkoci, *ACS Appl. Mater. Interfaces*, 2013, **5**, 1084.
- 97 S. Jayabal, R. Sathiyamurthi and R. Ramaraj, *J. Mater. Chem. A*, 2014, **2**, 8918.
- 98 G. Chen, Y. Jin, L. Wang, J. Deng and C. Zhang, *Chem. Commun.*, 2011, **47**, 12500.
- 99 Y. He, J. Tian, J. Zhang, S. Chen, Y. Jiang, K. Hu, Y. Zhao and S. Zhao, *Biosens. Bioelectron.*, 2014, **55**, 285.
- 100 C. Jing, L. Shi, X. Liu and Y.-T. Long, *Analyst*, 2014, **139**, 6435.
- 101 Y. Zhu, L. Xu, W. Ma, Z. Xu, H. Kuang, L. Wang and C. Xu, *Chem. Commun.*, 2012, **48**, 11889.
- 102 S. Chen, D. Liu, Z. Wang, X. Sun, D. Cui and X. Chen, *Nanoscale*, 2013, **5**, 6731.
- 103 R. Puk and J. H. Weber, *Anal. Chim. Acta*, 1994, **292**, 175.
- 104 Y. Li, C. Chen, B. Li, J. Sun, J. Wang, Y. Gao, Y. Zhao and Z. Chai, *J. Anal. At. Spectrom.*, 2006, **21**, 94.
- 105 M. B. Gholivand and M. H. Parvin, *Electroanalysis*, 2010, **22**, 2291.
- 106 K. Liu, N. Zhao and E. Kumacheva, *Chem. Soc. Rev.*, 2011, **40**, 656.
- 107 P. R. Sajanlal, T. S. Sreeprasad, A. K. Samal and T. Pradeep, *Nano Rev.*, 2011, **2**, 5883.
- 108 B. Goris, S. Bals, W. Van den Broek, E. Carbó-Argibay, S. Gómez-Graña, L. M. Liz-Marzán and G. V. Tendeloo, *Nat. Mater.*, 2012, **11**, 930.
- 109 E. Carbo-Argibay, B. Rodriguez-Gonzalez, I. Pastoriza-Santos, J. Perez-Juste and L. M. Liz-Marzan, *Nanoscale*, 2010, **2**, 2377.
- 110 O. A. Oviedo, E. P. M. Leiva and M. M. Mariscal, *Phys. Chem. Chem. Phys.*, 2008, **10**, 3561.
- 111 S.-Y. Zhang, M. D. Regulacio and M.-Y. Han, *Chem. Soc. Rev.*, 2014, **43**, 2301.
- 112 P. K. Jain, S. Eustis and M. A. El-Sayed, *J. Phys. Chem. B*, 2006, **110**, 18243.
- 113 P. R. Selvakannan, E. Dumas, F. Dumur, C. Péchoux, P. Beaunier, A. Etcheberry and C. R. Mayer, *J. Colloid Interface Sci.*, 2010, **349**, 93.
- 114 J.-M. Liu, H.-F. Wang and X.-P. Yan, *Analyst*, 2011, **136**, 3904.
- 115 H. H. Cai, D. Lin, J. Wang, P. H. Yang and J. Cai, *Sens. Actuators, B*, 2014, **196**, 252.
- 116 N. Bi, Y. Chen, H. Qi, X. Zheng, Y. Chen, X. Liao, H. Zhang and Y. Tian, *Sens. Actuators, B*, 2012, **166–167**, 766.
- 117 G. Chen, Y. Jin, W. Wang and Y. Zhao, *Gold Bull.*, 2012, **45**, 137.
- 118 M. Rex, F. E. Hernandez and A. D. Campiglia, *Anal. Chem.*, 2006, **78**, 445.
- 119 W. Chemnasiri and F. E. Hernandez, *Sens. Actuators, B*, 2012, **173**, 322.
- 120 G. S. Anand, A. I. Gopalan, S.-W. Kang and K.-P. Lee, *J. Anal. At. Spectrom.*, 2013, **28**, 488.
- 121 E. C. Heider, K. Trieu, A. F. Moore and A. D. Campiglia, *Talanta*, 2012, **99**, 180.
- 122 X. Niu, D. Xu, Y. Yang and Y. He, *Analyst*, 2014, **139**, 2691.
- 123 S. Wang, Z. Chen, L. Chen, R. Liu and L. Chen, *Analyst*, 2013, **138**, 2080.
- 124 Y.-J. Lan and Y.-W. Lin, *Anal. Methods*, 2014, **6**, 7234.
- 125 Z. Chen, R. Liu, S. Wang, C. Qu, L. Chena and Z. Wang, *RSC Adv.*, 2013, **3**, 13318.
- 126 S. Thatai, P. Khurana, S. Prasad and D. Kumar, *Microchem. J.*, 2014, **113**, 77.
- 127 Y. Liu, Y. Zhao, Y. Wang and C. M. Li, *J. Colloid Interface Sci.*, 2015, **439**, 7.
- 128 H. Huang, S. Chen, F. Liu, Q. Zhao, B. Liao, S. Yi and Y. Zeng, *Anal. Chem.*, 2013, **85**, 2312.
- 129 J. Xue, P. T. Lee and R. G. Compton, *Electroanalysis*, 2014, **26**, 1454.